SURVEYING TEMPERATURE AND DENSITY MEASUREMENTS IN NUCLEAR CALORIMETRY

G.RACITI[1], R.BASSINI[2], M.BEGEMANN-BLAICH[3], S.FRITZ[3], C.GROß[3], G.IMMÈ[1], I.IORI[2], U.LYNEN[3], M.MAHI[3], T.MÖHLENKAMP[3], W.F.J.MÜLLER[3], B.OCKER[3], T.ODEH[3], J.POCHODZALLA[3], G.RICCOBENE[1], F.P.ROMANO[1], A.SAIJA[1], C.SCHWARZ[3], V.SERFLING[3], M.SCHNITTKER[3], A.SCHÜTTAUF[3], W.SEIDEL[4], C.SFIENTI[1], W.TRAUTMANN[3], A.TRZCINSKI[5],G.VERDE[1], HONGFEI XI[3], B.ZWIEGLINSKI[5].

[1] *INFN Laboratori Nazionali del Sud and Sezione di Catania and Dipartimento di Fisica ed Astronomia dell' Università di Catania, Catania, Italy*

[2] *Dipartimento di Fisica, Università di Milano and I.N.F.N Milano, Italy*

[3] *Gesellschaft fur Schwerionenforschung, D-64291 Darmstadt, Germany*

[4] *Forschungszentrum Rossendorf, D-01314 Dresden, Germany*

[5] *Soltan Institute for Nuclear Studies, 00-681 Warsaw, Hoza 69, Poland*

E-mail: raciti@lns.infn.it

An experimental investigation on thermodynamical observables characterizing the conditions of multifragmenting systems is reported. High granularity hodoscopes allowed simultaneous measurements of isotopic and emission temperatures. HBT interferometry with light charged particles allowed radii measurements. The disagreement between the two temperature measurements could be related to the space-time evolution of the fragmentation process as confirmed by density measurements. The slope temperatures derived from the target spectator decay fragment energy spectra suggest a dependence on the Fermi motion within the initial system. The dependence of the Nuclear Caloric Curve on the mass of the systems was probed.

1 Introduction

One of the most intriguing phenomena observed in macroscopic systems is that of a phase transition. The exploration of the phase diagram of a substance is possible via calorimetric studies [1]. Indeed, from the correlation of the measured isotopic temperature [2] and excitation energy of projectile spectator in ^{197}Au+^{197}Au collisions at 600 AMeV, a caloric curve of nuclei has been reported [3]. The similarity of this curve to first-order liquid-gas phase transition in macroscopic systems has initiated a widespread activity, both theoretical and experimental in particular on the temperature measurements. In order to permit a cross comparison of different thermometers we measured simultaneously both isotope yields and particle-particle correlations from the decay of unstable states in the emitted fragments [4-7]. In a series of experiments we studied ^{197}Au + ^{197}Au collisions at 1

AGeV to investigate the spectator decay [4,8,9], and mid-central collisions at 50, 100, 150, and 200 AMeV [5] to study the decay of the participant region which is known to exhibit a considerable collective flow[10]. To investigate on system size dependence, we studied also central collisions $^{84}Kr+^{93}Nb$ at NSCL of MSU [6] at incident energies from 35 to 120 AMeV and $^{40}Ca+^{45}Sc$ at 40 AMeV at the LNS-Catania [7]. HBT interferometry technique was applied to charged particle relative momentum correlation functions in order to measure the size of the emitting systems [11] and densities were deduced once the system mass was determined. Moreover some discrepancies between the caloric curve of [3] with the ones obtained later by other groups [12-14] were suggested [15] to be related to the different masses of the studied systems. Recently a size dependence in the melting of sodium clusters has been reported [16].

2 Experimental Apparata

The experiments were performed at the SIS accelerator of the GSI, using the ALADiN facility, at the NSCL of MSU and at the LNS-Catania. In the GSI experiments [4,5,8,9] three modular hodoscopes each consisting of Si-CsI(Tl) telescopes(Si 3x3 cm^2 300μm thick, CsI scintillators 3x3 cm^2 6 cm long with photodiode readout), were set up with an angular resolution and granularity optimized to identify excited particle-unstable resonances in light fragments from the correlated detection of their decay products. A set of seven telescopes (Si 50 μm, 300 μm, and 1000 μm, CsI 4 cm long) at selected angles, measured the yields of isotopically resolved light fragments. At 1 AGeV the impact-parameter selection was achieved by measuring the quantity Z_{bound} (the sum of all Z>1 belonging to the projectile) through the forward angles TOF wall of the ALADiN setup [17]. At lower bombarding energies the associated charged particle multiplicity was sampled, at forward angles, with an array of 36 CaF_2-plastic phoswich telescopes (ZDO) and with a set of 6 Si-strip 16-fold detectors 300 μm thickness, 5×5 cm^2 surface. At the LNS laboratory we studied the $^{40}Ca + ^{45}Sc$ reaction at 40AMeV with a similar setup [7,15]. Two high granularity hodoscopes were used to measure simultaneously particle-particle correlations and the yields of isotopically resolved fragments. One, the HODO-CT was the same 96 element hodoscope used at the GSI, improved with a 50 μm Si-detector in front of each telescope, in order to reduce the detection threshold. The other, HODO-FWD, covered the angular range $\theta_{lab} = 5° \div 11°$ around zero degree in order to detect projectile fragmentation. It was composed by 80 two-folds telescopes (Si 300 μm 1×1 cm^2 followed by a 10 cm long CsI(Tl)) and 40 three-folds telescopes of the same kind as the HODO-CT's ones. Charged particle multiplicity was sampled by a set of 12 Si strip detectors 16-folds set up around the target. At the NSCL the $^{84}Kr+^{93}Nb$ reaction , was studied [6] by coupling the HODO-CT with the 4π detector (Soccer Ball) that served as impact parameter filter .

3 Nuclear Thermometers Cross Comparison.

The methods currently in use to measure temperature of nuclear systems are summarized in Fig. 1-a [1]. In particular the Caloric Curve of Ref.[3] was built by correlating excitation energy with "isotope" temperature, i.e. the one deduced from the double ratio of isotopes differing by one mass unit[2]. Indication for equilibrium in the spectator system is related to the universality with respect to the colliding systems and the incident energy [18] and to a good agreement with the statistical multifragmentation models[19].However, several both theoretical and experimental works appeared on the problems related to the influence of sequential decay [20,21] and the different values measured depending on the selected isotope pairs[22,23]. Nevertheless, "isotope" temperatures seem to well reflect the breakup conditions. In Fig. 1-b the results for T_{HeLi} in ^{197}Au on ^{197}Au spectator fragmentation, obtained in three different measurements, are shown as a function of Z_{bound}. Integrated yields of ^{3,4}He and ^{6,7}Li isotopes were measured, for the projectile-spectator breakup at forward angles by the ALADIN spectrometer, and for the target spectator, by a standard moving source fit procedure of the energy spectra measured in the backward region with the four-element telescopes.In both cases Z_{bound} was determined from the coincident projectile fragments detected by the ALADINsetup.

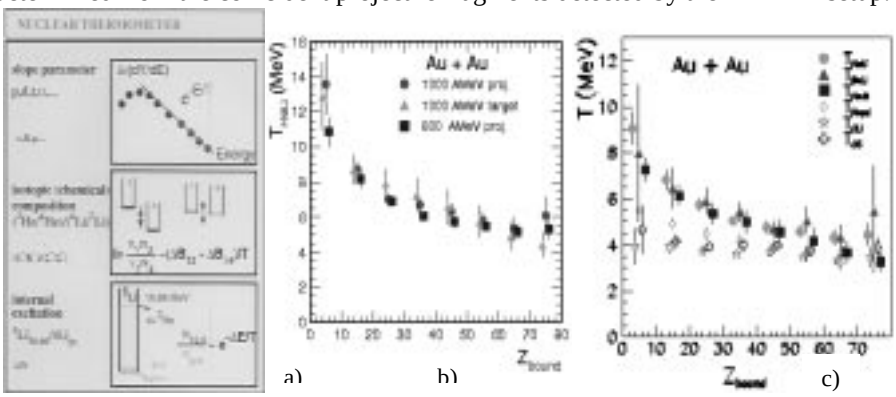

Figure 1 : a) Nuclear thermometers. b) Temperatures T_{HeLi} for target (E=1000 A MeV) and projectile spectators (E=600 and 1000 A MeV) as a function of Z_{bound}. c) QSM-corrected isotope temperatures for ^{197}Au target spectator at E=1000 A MeV as a function of Z_{bound} .

In Fig.1-c results are given for a variety of isotope thermometers that are all characterized by a double difference of the binding energies $\Delta B>10$MeV. All values have been corrected [1] for the effect of secondary decays by using the predictions of the quantum statistical model (QSM) [24].The rise at small Z_{bound}, i.e. high excitation energy, already observed for T_{HeLi} ,is well reproduced by both $T_{H,He}$ and T_{BeLi} (^{7,9}Be and ^{6,8}Li isotope ratios). This demonstrates that the rise is not necessarily related to a particular behavior of either ^{3}He or ^{4}He and is not very much affected by the sequential feeding for the quoted thermometers.

3.1 Emission vs. Isotope Temperatures.

In order to permit a cross comparison of two different thermometers we measured, for the same class of events of the same fragmenting system, both "isotope" and "emission" temperatures. The latter can be calculated assuming that the states of the decaying fragments are populated according to a Boltzmann law. Therefore from peaks in relative momentum correlation functions due to resonant decay of two coincident particles, acceptance corrected yields of fragments excited states have been determined [5].
Figure 2 shows the comparison of the isotope and emission temperatures measured in central collisions in the Au+Au and Kr+Nb reactions at different incident energies. Differences up to 8 MeV between the two thermometers are reached at the highest bombarding energy. We notice that temperatures related with Carbon isotopes (T_{CLi}, T_{CC}) show the same behavior of the emission ones (Fig.s.1-c,2-b)

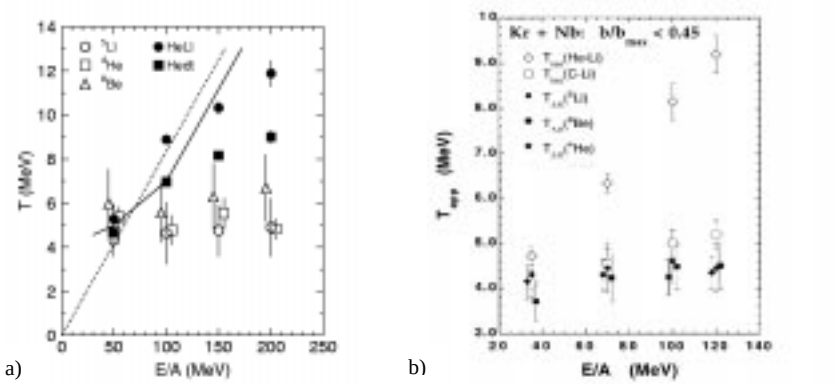

Figure 2: a) Emission temperatures extracted from the excited states of ^{4}He, ^{5}Li, ^{8}Be and isotope temperature are shown as a function of the bombarding energy for central Au+Au collisions [5]. b) Same for Kr+Nb central collisions [6].

Emission temperatures measured by fragments excited states populations should be related to a later time when the adiabatic expanding system has cooled down[5,15]. A different freeze-out time of the chemical degree of freedom and the internal ones of the single constituents could explain the observed different behavior.

3.2 Kinetic Energy Spectra.

Energy spectra of charged particles and fragments measured in the ^{197}Au + ^{197}Au target spectator fragmentation at 1 AGeV exhibit Maxwellian shapes to a good approximation [8,9]. The slope parameters, shown in Fig.3-a, apart for protons, are scattered closely around a mean value of 17 MeV. A constant temperature and the corresponding mass invariance of the mean kinetic energies is a very general indication of equilibrium.

Since the mutual Coulomb repulsion after breakup and the small but finite motion of the target spectator have relatively small contributions and, at backward angles, should cancel each other, the measured slope parameters of T≈17 MeV may be taken as representative of the thermal component of the fragment kinetic energies [9]. However, as it was suggested by Goldhaber [25], the large kinetic energies of fast-fragmentation products may have their origin in the nucleonic Fermi motion and the resulting behavior is indistinguishable from that of a thermalized system with rather high temperature. Goldhaber's idea has been extended by Bauer [26] to the case of expanded fermionic systems at finite temperatures. The slope temperatures, represented by lines in Fig. 3-b, calculated assuming the measured breakup temperatures T_{HeLi} as the system temperature and the two values ρ/ρ_0= 1.0 and 0.3 ,for the breakup density, are in the range of the experimental values. They reproduce the rise with decreasing Z_{bound} which follows as a consequence of the rising breakup temperature T_{HeLi}. It also seems that a better agreement favor the prediction for ρ/ρ_0 = 1.0.

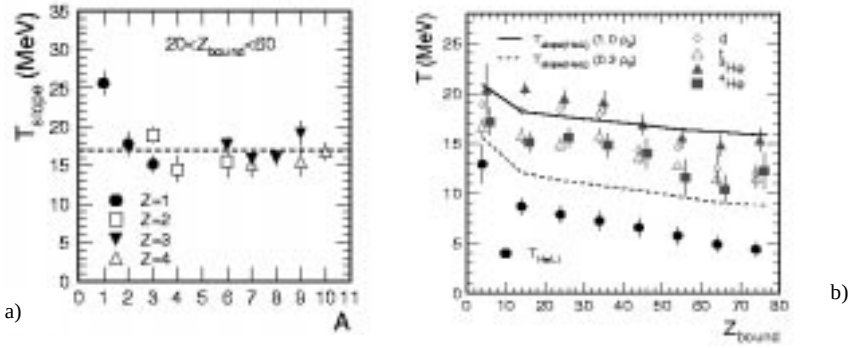

Figure 3: a) Slope temperatures measured in the ^{197}Au + ^{197}Au reaction at E = 1000 A MeV, as a function of the fragment mass number A. b) Slope temperatures for light charged particles and the isotope temperature T_{HeLi} as a function of Z_{bound}.

This result suggests a fast abrasion stage that will induce fragmentation of the remaining spectators but do not affect much the Fermi motion of the constituent nucleons in the equilibrated system before its decay. This is consistent with a partitioning according to phase space but contradicts the equilibration of the kinetic degrees of freedom at the breakup that is assumed in the statistical multifragmentation models [24].

4 Density measurements

The density value ρ/ρ_0 , used to study slope temperatures in the previous section, was measured in ^{197}Au + ^{197}Au target spectator fragmentation at 1 A GeV [4] by means of particle-particle HBT interferometry [11]. Details on the analysis of the

particle-particle correlation functions, sorted into bins of Z_{bound} in order to select excitation energy and impact parameter, are given in [27]. Radii were deduced in the zero-lifetime limit for the source, and densities were calculated by dividing the number of spectator constituents evaluated from Z_{bound} [3,4] by the source volume. The derived densities (Fig.4-a) vary considerably with impact parameter, roughly in proportion to the variation of the spectator mass. In the p-p case, the mean relative densities decrease from $\rho/\rho_0 = 0.4$ for the near-peripheral to below $\rho/\rho_0 = 0.2$ for the most central collisions [4]. These values compare well with the densities assumed in the statistical multifragmentation models [24] in contrast with the $\rho/\rho_0=1$ value suggested by the slope temperatures analysis. The lower values related to the p-α and d-α correlations may be partially due to the different formalisms that were used but they could indicate a moderate expansion of the system.

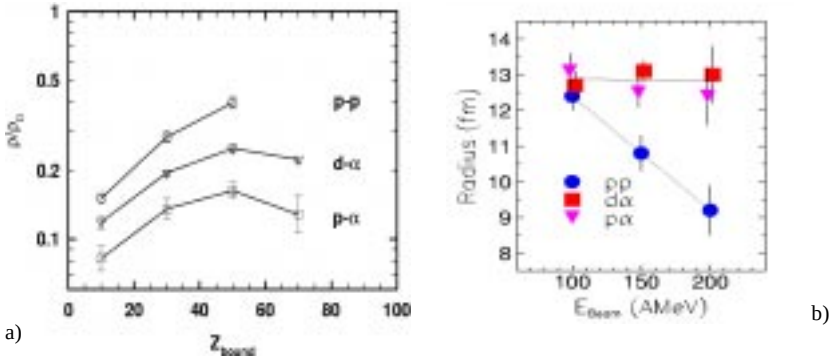

Figure 4: a) Breakup density ρ/ρ_0 as deduced from p-p, p-α, and d-α correlation functions for ^{197}Au + ^{197}Au collisions at 1000 A MeV per nucleon. The error bars represent the statistical uncertainty. b) Radii extracted from p-p, pα and dα correlation functions [15,28].

Similar differences are evidenced in the analysis of the proton-proton and unlike particle correlations measured in Au+Au central collisions. The collective expansion, that represents, in central collisions, a significant fraction (about 40%) of the energy available in the center-of-mass frame [10], was taken into account in the radii determination from the experimental correlation functions. In fig.4-b the constant values measured from pα and dα contrast with the ones from p-p that drop with increasing beam energy. These differences, enhanced by the increasing of the collective radial flow, could be related to the lower density reached by the expanding system at the freeze-out time, when alpha correlations sample the emitting source. This scenario agrees well with the EES [29] prediction that the emission time for α's and larger clusters is delayed with respect to p, d, t, and ^{3}He. Moreover, since an adiabatic expansion imply the cooling of the system, it may not be too surprising that the discrepancy between the isotope and emission thermometers arises at beam energies where collective radial flow becomes important. The time evolution of the system is emphasized by the saturation of the

excited-state temperatures, radii and fragments emission time measured in Ref.[30]. The saturation temperature T≈5 MeV is similar to the asymptotic temperature obtained in dynamical models describing the reaction process [31].

5 Caloric curve as an image of the finite size

An intriguing problem is related to the different behavior of the ALADiN Caloric Curve [3] and the one obtained by the INDRA Collaboration studying the ^{40}Ar projectile fragmentation at 95 A MeV incident energy[12]. Fig. 5-a shows a comparison between these caloric curves and the isotope temperature T_{HeLi} measured in central collisions ^{84}Kr+^{93}Nb at different energies [6] and in ^{40}Ca+^{45}Sc at 40 A MeV [7].
The excitation energy for the ^{84}Kr+^{93}Nb central collisions were evaluated roughly from the C.M. available kinetic energy reduced by the collective radial expansion term deduced from the systematics [10]. The intermediate source excitation energy in ^{40}Ca+^{45}Sc was evaluated considering the complete transfer of the available kinetic energy to an incomplete fused system of 82 nucleons, as suggested from the C.M. velocity spectra fit [7]. We notice that the same excitation energy (E/A≈8MeV) determines higher temperature in the system produced in the ^{40}Ca+^{45}Sc (A=82) than in the A≈170 system selected in ^{84}Kr+^{93}Nb at 35 AMeV incident energy.

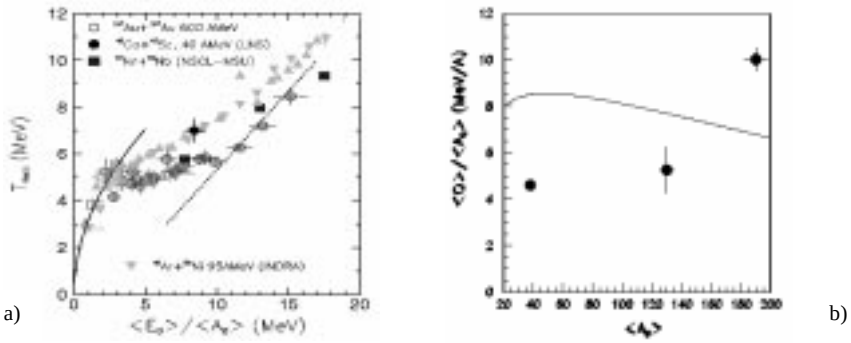

Figure 5: a) Cross comparison between caloric curves of nuclei and b) the related latent heat/nucleon.[7]

The comparison suggests a size dependence of the temperature-excitation energy correlation. The same indication is given by the latent heat reported in Fig 5-b versus the mass of the investigated systems. The latent heat values were deduced from the caloric curves of [3] [12] and [13] by integrating the gaussian shapes of the $\delta E / \delta T$ functions around the transition temperature[7]. The increasing values with the system mass are inconsistent with a volume dependence (curve in fig 5-b).
Recently [16] surprisingly large variations in the melting point and latent heat have been observed with changing cluster size of ionized sodium atoms. These variations

cannot be yet fully explained theoretically, and refer to different microscopic structures and phase transitions, but we want to emphasize that a size dependence of the thermodynamical properties of different systems opens the possibility of precise studies on finite systems far away from the infinite size limit.

References

1. J.Pochodzalla, Prog.Part.Nucl.Phys. 37(1997)443 and references therein
2. S.Albergo et al., *Il Nuovo Cimento* **89A** (1985) 1.
3. J.Pochodzalla et al., *Phys. Rev. Lett.* **75** (1995) 1040.
4. S. Fritz et al., *Phys. Lett. B* **461**(1999)315.
5. V. Serfling et al., *Phys. Rev. Lett*. **80** (1998) 3928.
6. H. Xi et al., *Phys. Rev. **C*** **58** (1998)2636.
7. C.Sfienti, *PHD Thesis* -Univ Catania 2000
8. Hongfei Xi et al., *Z.Phys.* **A359** (1997)397.
9. T. Odeh et al., *Phys. Rev. Lett*. **84** (2000)4557.
10. W.C.Hsi et al., *Phys. Rev. Lett*. **73**(1994)3367 and M.A. Lisa et al., *Phys. Rev. Lett.* **75**(1995)2662 and G. Poggi et al., *Nucl. Phys.* **A586**(1995)755.
11. S.E. Koonin, *Phys. Lett.* **B70**(1977)43, D.H.Boal et al. *Rev. Mod. Phys.* **62** (1990) 553
12. Y.G..Ma et al., *Phys. Lett*. B390(1997)41.
13. G.Auger et al. *Proceedings of CRIS 96* Ed.World Scientific (1996), 133
14. J.A.Hauger et al. *Phys Rev Lett*. **77**(1996) 235
15. G.Raciti et al. *Nuovo Cimento* **A111**(1998)987
16. M. Schmidt et al., *Nature* **393** (1998)238.
17. J. Hubele et al., *Z.Phys*. **A340** (1991)263.
18. A.Schüttauf et al., *Nucl. Phys.* **A607** (1996)457.
19. A.Botvina et al. , *Nucl Phys.* **A584** (1995) 737
20. M.B. Tsang et al., Phys.Rev.Lett 78(1997)3836.
21. H.Xi et al. *Phys. Rev.* **C59** (1999) 1567
22. A.Siwek,et al *Phys. Rev.* **C57** (1998) 2507
23. H.Raduta, R.Raduta *Proceedings of this Conference*
24. D.H.E.Gross, *Rep. Prog. Phys.* **53** (1990)605, J.P.Bondorf et al., *Nucl. Phys.* **A444** (1985)460. J.P.Bondorf et al., *Phys Rep*. **257**(1995)133.
25. A.S. Goldhaber, *Phys.Lett.* **B53** (1974)306.
26. W. Bauer, *Phys.Rev.* **C51**(1995)803.
27. C.Schwarz et al. *Proceedings of this Conference*
28. G.Immè et al. *Proceedings of CRIS 98* Ed.World Scientific (1999) 289
29. W.A. Friedmann, *Phys. Rev.* **C42** (1990)667
30. E.Bauge et al. *Phys Rev Lett*. **70** (1993) 3705
31. C. Fuchs et al., *Nucl. Phys.* **A 626** (1997)987.